

EVOLUTION OF PHENOTYPIC CLUSTERS THROUGH COMPETITION AND LOCAL ADAPTATION ALONG AN ENVIRONMENTAL GRADIENT

Olof Leimar,^{1,2} Michael Doebeli,^{3,4} and Ulf Dieckmann^{5,6,7}

¹*Department of Zoology, Stockholm University, SE-10691 Stockholm, Sweden*

²*E-mail: olof.leimar@zoologi.su.se*

³*Department of Zoology and Department of Mathematics, University of British Columbia, 6270 University Boulevard, Vancouver, BC, Canada*

⁴*E-mail: doebeli@zoology.ubc.ca*

⁵*Evolution and Ecology Program, International Institute for Applied Systems Analysis, Schlossplatz 1, A-2361 Laxenburg, Austria*

⁶*Section Theoretical Biology, Institute of Biology, Leiden University, Kaiserstraat 63, NL-2311 GP Leiden, The Netherlands*

⁷*E-mail: dieckmann@iiasa.ac.at*

Received July 31, 2007

Accepted January 16, 2008

We have analyzed the evolution of a quantitative trait in populations that are spatially extended along an environmental gradient, with gene flow between nearby locations. In the absence of competition, there is stabilizing selection toward a locally best-adapted trait that changes gradually along the gradient. According to traditional ideas, gradual spatial variation in environmental conditions is expected to lead to gradual variation in the evolved trait. A contrasting possibility is that the trait distribution instead breaks up into discrete clusters. Doebeli and Dieckmann (2003) argued that competition acting locally in trait space and geographical space can promote such clustering. We have investigated this possibility using deterministic population dynamics for asexual populations, analyzing our model numerically and through an analytical approximation. We examined how the evolution of clusters is affected by the shape of competition kernels, by the presence of Allee effects, and by the strength of gene flow along the gradient. For certain parameter ranges clustering was a robust outcome, and for other ranges there was no clustering. Our analysis shows that the shape of competition kernels is important for clustering: the sign structure of the Fourier transform of a competition kernel determines whether the kernel promotes clustering. Also, we found that Allee effects promote clustering, whereas gene flow can have a counteracting influence. In line with earlier findings, we could demonstrate that phenotypic clustering was favored by gradients of intermediate slope.

KEY WORDS: Asexual populations, Allee effects, disruptive selection, parapatry, pattern formation, quantitative characters.

The evolution of a quantitative trait along an environmental gradient is a topic of interest to population genetics and evolutionary ecology (Slatkin 1978; Kirkpatrick and Barton 1997; Barton 1999; Case and Taper 2000), and is connected to the classi-

cal study of gene frequency clines (Haldane 1948; Fisher 1950; Bazykin 1969; Endler 1977). When there is stabilizing selection on a quantitative trait toward a spatially varying optimum, together with gene flow between nearby locations, the traditional

expectation has been that gradual variation in the optimum ought to be mirrored by a gradual and, owing to gene flow, equally smooth or even smoother variation in the average value of the trait.

A contrasting perspective was put forward by Doebeli and Dieckmann (2003), who argued that frequency-dependent competition in trait space and local competition in geographical space, acting together with stabilizing selection along an environmental gradient, can create discrete clusters in the distribution of a trait, despite the counteracting effects of gene flow. Doebeli and Dieckmann (2003) claimed that this cluster formation could occur even when frequency-dependent competition would not give rise to disruptive selection in a spatially unstructured, well-mixed population. They emphasized the possible significance of such a process for parapatric speciation, extending earlier work (Dieckmann and Doebeli 1999) that dealt with the possible significance of evolutionary branching (Metz et al. 1992, 1996; Geritz et al. 1998) for sympatric speciation. Our aim here is to shed further light on the evolution of phenotypic clusters along environmental gradients by investigating the causes of phenotypic pattern formation.

The conclusions of Doebeli and Dieckmann (2003) were challenged by Polechová and Barton (2005), who approximated the original individual-based stochastic model by a deterministic reaction–diffusion model. Using Gaussian competition kernels in their approximate model, Polechová and Barton (2005) argued that a gradual environmental cline will lead to gradual variation in a quantitative trait. They suggested that the clustering observed in the analysis of asexual evolution by Doebeli and Dieckmann (2003) was caused by the boundary conditions of the model. In line with earlier findings (e.g., Sasaki 1997), our analysis here confirms that Gaussian competition kernels in themselves are not sufficient to cause clustering, but our overall conclusions are quite different from those reached by Polechová and Barton (2005). In particular, we identify parameter regions of our model in which clustering is a robust outcome, and we show that this outcome does not depend on particular boundary conditions. To investigate cluster formation without an impact of boundary effects, we study a hypothetical, infinitely extended environmental gradient and analyze the conditions for periodic clustering along this gradient.

Using an asexual, deterministic model, we investigate the importance of two different factors for the formation of phenotypic clusters, namely the shape of competition kernels and the strength of Allee effects. There has been a long and influential tradition in ecological modeling to focus on special types of competition kernels, mainly Gaussian and biexponential competition functions (e.g., Roughgarden 1972, 1979; MacArthur 1972; May 1973), which was motivated more by mathematical convenience than by

biological realism. A basic aim of our analysis is to provide general insights into the consequences of going beyond this simplifying assumption.

An important aspect of our treatment is that we identify a general property characterizing the shape of competition kernels that promote pattern formation. The crucial property is the sign structure of the Fourier transform of the kernel, in agreement with the analysis of a situation without spatial variation by Pigolotti et al. (2007). If the Fourier transform is nonnegative, as is the case for a Gaussian, the kernel does not by itself cause clustering in models of the type studied here. In contrast, if the transform changes sign to negative values, the kernel shape can induce pattern formation. We provide an intuitive interpretation of this condition, in terms of how the intensity of competition depends on distance in trait space or geographical space.

We also included Allee effects in our analysis. These are among the most-studied phenomena in population biology and are well known for their potential to create spatial variation in abundance (Gyllenberg et al. 1999; Keitt et al. 2001) and to promote species coexistence (Hopf and Hopf 1985). Allee effects are often considered as consequences of the discreteness of individuals, such as when suitable mates or conspecific cooperators become locally rare. It is therefore natural to investigate the influence of Allee effects on phenotypic pattern formation along an environmental gradient. In our analysis, we focus on so-called weak Allee effects, through which a population's per capita growth rate is reduced, but still remains positive at low population density.

With these ingredients, we present results from a numerical analysis of the model and from an analytical approximation in the form of a reaction–diffusion equation. Our analytical approximation is accurate in the low-mobility limit. The importance of the approximation lies in providing a qualitative understanding of the causes of phenotypic pattern formation, which show interesting similarities to the processes giving rise to Turing patterns (Turing 1952). To illustrate the interplay of environmental gradients of different slopes with competition acting locally in trait space or geographical space, we present results for parameter ranges in which stabilizing selection on the trait is stronger than the diversifying influence of competition in trait space. In a spatially uniform and well-mixed situation, such conditions would give rise to a unimodal distribution of trait values (Geritz et al. 1998; Dieckmann and Doebeli 1999), which means that the phenotypic clustering observed in our analysis is gradient induced. We discuss our results in relation to previous work, including the results of Doebeli and Dieckmann (2003), and summarize how the conditions for clustering along environmental gradients obtained in our analysis may help understand patterns in real populations.

Methods

MODEL DESCRIPTION

The analysis of Doebeli and Dieckmann (2003) rested on the numerical investigation of an individual-based stochastic model. Here we instead use the idealization of a (locally) large population and treat population dynamics deterministically, in terms of continuously varying local densities. The same assumption is used in traditional reaction–diffusion models. In contrast to these, however, we start out by describing movements in geographical space and mutations in trait space through explicit kernels, thereby avoiding the limitations of diffusion approximations.

We consider an asexual population with a one-dimensional quantitative trait u . The population lives along an environmental gradient, with the one-dimensional coordinate x indicating spatial position. We use $n(u, x, t)$ to denote the local density of individuals with trait u and location x at time t (below, we usually refrain from making the argument t explicit). The density n has the deterministic dynamics

$$\begin{aligned} \frac{\partial}{\partial t} n(u, x) = & [1 - n_c(u, x)/K(u, x) - d(\bar{n}(x))] n(u, x) \\ & + v_\mu [n_\mu(u, x) - n(u, x)] \\ & + v_m [n_m(u, x) - n(u, x)]. \end{aligned} \quad (1)$$

This equation describes the change over time of the local density, under the influence of births, deaths, trait mutation, and movement in space. A brief description of the terms appearing on the right-hand side of equation (1) is as follows (see also Doebeli and Dieckmann 2004). The time scale is chosen so as to imply a per capita birth rate equal to 1. The birth rate is offset by the per capita death rate resulting from competition, expressed as the ratio of an effective competitive density $n_c(u, x)$ and a local carrying capacity $K(u, x)$ measured on the density scale, and the death rate from an Allee effect $d(\bar{n}(x))$, which becomes small as the total local density,

$$\bar{n}(x) = \int n(u', x) du',$$

increases. The two last terms on the right-hand side of equation (1) represent trait mutation and spatial movement with per capita rates v_μ and v_m , and $n_\mu(u, x)$ and $n_m(u, x)$ are the densities immediately after mutation and movement, respectively.

The carrying capacity $K(u, x) = \kappa(u - gx)$ is assumed to be unimodal with a maximum at a trait value $u = gx$ that changes linearly with a slope g along the environmental gradient. We refer to the line $u = gx$ as the environmental cline. Choosing the scale of population density so that the maximum of K equals 1, we use a Gaussian carrying capacity,

$$K(u, x) = \kappa(u - gx) = \exp[-\frac{1}{2}(u - gx)^2/\sigma_K^2],$$

and set $\sigma_K^2 = 1$ as a choice of scale for u . The intensity of competition depends on the effective density experienced by phenotype u at location x ,

$$n_c(u, x) = \iint a_0(u' - u) a_1(x' - x) n(u', x') du' dx',$$

which is obtained as a weighted average, with the phenotypic competition kernel a_0 and the spatial competition kernel a_1 weighting the competitive impact of other individuals. These kernels have symmetric shapes, integrals normalized to 1, and variances σ_0^2 and σ_1^2 , respectively. As a choice of scale for x we set $\sigma_1 = 1$. The phenotypic and spatial competition kernels describe how the strength of competition varies with phenotypic and spatial distance, and they play important roles in our analysis. Because the shapes of the competition kernels can influence pattern formation, we make use of a family of kernels formed as convolutions of a Gaussian with a box-shaped kernel (a uniform distribution on a finite, symmetric interval), allotting different proportions of the total variance to these components. This results in more or less box-like kernels, as illustrated in Figure 1. The Allee effect $d(\bar{n}(x))$ is assumed to have the form

$$d(\bar{n}) = d_0 \exp(-\bar{n}/n_0),$$

with parameters $0 < d_0 < 1$ and $n_0 > 0$. This corresponds to a so-called weak Allee effect (Wang and Kot 2001; Taylor and Hastings 2005), which entails a reduced but positive population growth rate of $1 - d(\bar{n}(x))$ even at low local densities \bar{n} . The rates of increase in local density from mutation and movement are

$$\begin{aligned} v_\mu n_\mu(u, x) &= v_\mu \int b_\mu(u' - u) n(u', x) du', \\ v_m n_m(u, x) &= v_m \int b_m(x' - x) n(u, x') dx', \end{aligned}$$

where, respectively, v_μ and v_m are per capita rates of trait mutation and spatial movement and b_μ and b_m are mutation and movement kernels. These kernels are Gaussian with zero means and variances σ_μ^2 and σ_m^2 , respectively. The last two terms on the right-hand side of equation (1) then represent balances between the increase and decrease in density from mutation and movement events.

NUMERICAL ANALYSIS

To investigate the evolution of phenotypic clusters we integrated equation (1) numerically, looking for solutions with “cline periodicity,” that is, that satisfy the condition $n(u + gp, x + p) = n(u, x)$ for all x , where p is the period in geographical space, with the corresponding period gp in trait space (Fig. 2A below shows a cline-periodic solution). The condition of cline periodicity applies to a cline $u = gx$ with a given slope g . A solution is called “cline-like” if it has the form $n(u, x) = \eta(u - gx)$ for some function η , and such a solution will be cline periodic for any period p . For a cline-like solution, the shape is given by $\eta(u)$ and remains constant across geographical space when viewed relative to the

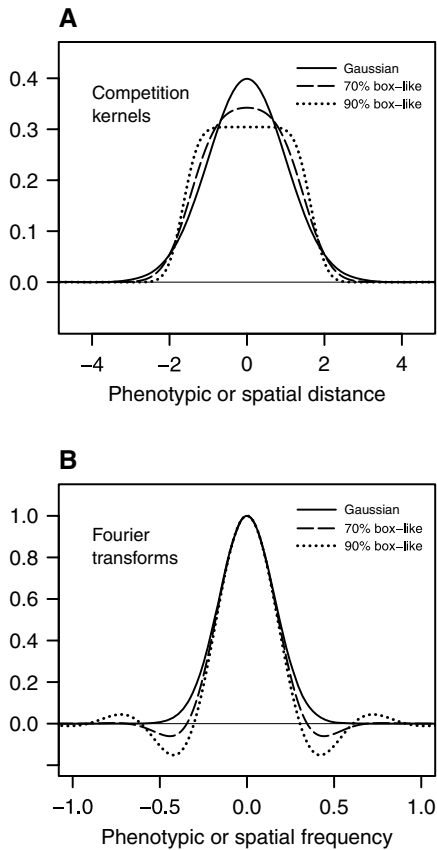


Figure 1. Examples of competition kernels. (A) Three competition kernels, each with variance 1. The 70% and 90% box-like kernels are obtained as convolutions of a uniform distribution on a finite, symmetric interval, with variance 0.7 or 0.9, and a Gaussian with corresponding variance 0.3 or 0.1. (B) Fourier transforms of the three kernels. The Fourier transform of a Gaussian is a Gaussian, and thus remains positive for all frequencies, whereas the Fourier transform of a box-like kernel has tails that oscillate in sign. The amplitude of these oscillations increases as the kernel's shape becomes more box-like. The negative values of a Fourier transform can induce pattern formation, and the spatial frequencies at which the Fourier transform is negative determine the spatial scale of patterning. Fourier transforms of wider competition kernels are narrower, as the width of the Fourier transform is inversely proportional to the width of the kernel.

environmental cline (Fig. 2B below shows a cline-like solution). Our approach is to first determine a cline-like equilibrium solution for a given set of parameter values and then to investigate the stability of this solution by introducing small cline-periodic perturbations with different spatial periods p . This is essentially the method used by Turing (1952) to study pattern formation. Using a search algorithm (golden section search; Press et al. 1992), we identified the spatial period having the highest rate of exponential growth λ in the deviation from the cline-like equilibrium.

Intuitively, our approach corresponds to studying an (hypothetical) infinitely extended environmental gradient (given by the

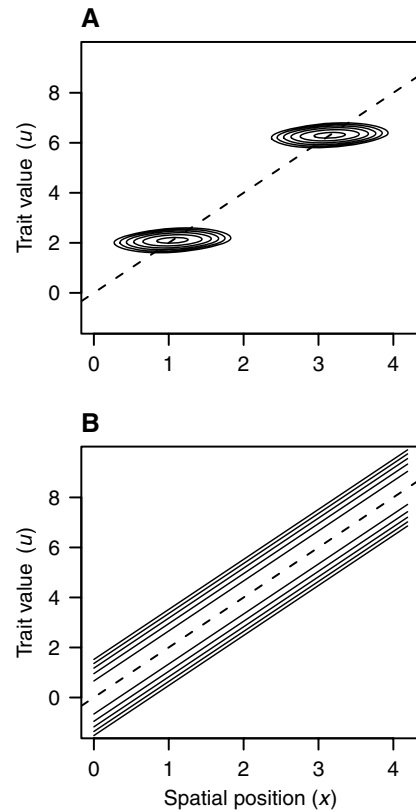


Figure 2. Stable equilibrium solutions. The contour plots show densities $n(u,x)$ of solutions to equation (1) for an environmental cline with slope $g = 2$, indicated by the dashed lines. (A) When the competition kernels in trait space and geographical space both have the 90% box-like shape shown in Figure 1, there is clustered stable equilibrium, shown in the figure, whereas the cline-like equilibrium solution to equation (1) is unstable. The instability of the cline-like solution is most pronounced for the illustrated spatial period of $p = 2.10$ in geographical space, with a corresponding period of $gp = 4.20$ in trait space (two whole periods are shown in the plot, whereas the model's domain in x and u is infinitely extended). The contour lines indicate density levels, varying from 0.001 to 100 with even logarithmic spacing; the maximum density is 247.6. The plot shows the density at $t = 5000$, when a stable equilibrium has been reached. The solution to equation (1) is relatively close to this equilibrium already at time $t = 200$. (B) When the competition kernels instead have Gaussian shapes, the cline-like equilibrium solution to equation (1) is stable. The contour lines indicate density levels at time $t = 200$, varying from 0.0001 to 1 with even logarithmic spacing; the maximum density is 8.50. For both plots, the initial density at time $t = 0$ was given by a very slight, oscillating perturbation ($\epsilon = 0.001$) of the cline-like equilibrium solution. Other parameter values: $\sigma_K = 1$, $\sigma_0 = 2$, $\sigma_1 = 1$, $\alpha_0 = 0$, $\nu_\mu = 0.01$, $\sigma_\mu = 0.05$, $\nu_m = 1$, and $\sigma_m = 0.05$.

cline $u = gx$ with x ranging from minus infinity to infinity and a corresponding infinite range of trait values u), by investigating the stability of solutions to equation (1) for which the density $n(u,x)$ is constant along the cline. Such a cline-like equilibrium is unstable if

density perturbations with certain spatial periods tend to increase in magnitude over time. If spatially periodic fluctuations grow, one may expect that the solution eventually approaches some stable cline-periodic equilibrium with a clustering of the density $n(u,x)$. In these cases we are interested in the properties of the clustered equilibrium. Further details on the numerical procedures are given in the Appendix.

APPROXIMATE ANALYTICAL TREATMENT

For small mutational increments and movement steps (small σ_μ^2 and σ_m^2), equation (1) can be approximated by a reaction–diffusion equation with small diffusion coefficients (see Appendix). When stabilizing selection is stronger than the diversifying influence of competition in trait space (i.e., when $\sigma_K^2 < \sigma_0^2$), we expect an equilibrium solution for which the trait distribution is concentrated along the cline $u = gx$. Furthermore, if the fitness landscape is approximately quadratic for small deviations from the cline, we expect the density to have a Gaussian shape, leading to an expression of the form

$$n(u, x) \approx (N_0 + N_1\sigma^2) \frac{1}{\sqrt{2\pi\sigma^2}} \exp[-\frac{1}{2}(u - gx)^2/\sigma^2], \quad (2)$$

where σ^2 approaches zero when σ_μ^2 and σ_m^2 approach zero. The intuition behind this expression is that in the limit of no mutation and no mobility, a cline of Dirac delta peaks, $N_0\delta(u - gx)$, will be an equilibrium solution. Small mutations and, for $g > 0$, mobility between nearby positions in space have the effect of broadening the delta peaks, turning them into narrow Gaussians with variance σ^2 . At the same time, total population density changes linearly in σ^2 , from N_0 to $N_0 + N_1\sigma^2$, under the combined influence of greater mortality from stabilizing selection and less mortality from competition for a distribution that is more spread out along the trait axis. Note also that the density in equation (2) is cline-like. Expressions giving the equilibrium values of the parameters N_0 , N_1 , and σ^2 are derived in the Appendix.

To determine the stability of the cline-like equilibrium given by equation (2), we can study solutions of the form

$$n(u, x) \approx [N_0 + N_1\sigma^2 + w(x, t)] \frac{1}{\sqrt{2\pi\sigma^2}} \exp[-\frac{1}{2}(u - gx)^2/\sigma^2]. \quad (3)$$

If $w(x,t)$ is a periodic function of x with period p , the density in equation (3) will be cline-periodic. The stability of the corresponding cline-like equilibrium in equation (2) means that no small perturbation $w(x,t)$ of period p will grow, for any choice of p , which in turn depends on how competition, the Allee effect, and mobility affect the deviation from a cline-like equilibrium. For densities concentrated along the cline $u = gx$, competitive effects along the cline can be described by a competition kernel

$$\alpha(x) = \frac{1}{C} a_0(gx) a_1(x),$$

where the normalization constant C appears in the denominator to give α an integral equal to 1. We can derive an approximate reaction–diffusion equation for $w(x)$, in which the kernel $\alpha(x)$ appears (see Appendix), and this equation can be used to investigate if perturbations having period p will grow or decay. The stability analysis is most conveniently performed using Fourier analysis. A period p corresponds to a spatial frequency $\phi = 1/p$ and the aim of the analysis is to determine if a Fourier component of w with spatial frequency ϕ will grow or decay. The approach of examining Fourier components to investigate pattern formation was originally used by Turing (1952) and has subsequently been widely applied to that end (Okubo et al. 2001), also in the context of populations competing for resources (e.g., Roughgarden 1972; Bolker and Pacala 1997; Sasaki 1997). For the analysis we need the Fourier transform of the kernel $\alpha(x)$, which is given by

$$\tilde{\alpha}(\phi) = \int \alpha(x) \exp(-i2\pi\phi x) dx,$$

where ϕ is a spatial frequency and i is the imaginary unit. It is shown in the Appendix that a Fourier component of w with spatial frequency ϕ will grow at the rate

$$\lambda(\phi) = -N_0 C \tilde{\alpha}(\phi) - N_0 d'(N_0) - m(2\pi\phi)^2, \quad (4)$$

where d' is the derivative of the Allee effect function and $m = \nu_m \sigma_m^2 / 2$ is a diffusion coefficient describing mobility in geographical space.

If there are spatial frequencies for which the growth rate λ in equation (4) is positive, the cline-like equilibrium will be unstable with respect to perturbations containing such spatial frequencies. The following three points summarize properties of equation (4). First, the last term of equation (4), describing the effect of mobility, becomes increasingly negative as the spatial frequency ϕ increases, which promotes stability more and more strongly. Second, in the absence of an Allee effect ($d_0 = 0$), the growth rate λ is negative at $\phi = 0$, because $\tilde{\alpha}(0) = 1$ holds ($\tilde{\alpha}(0) = \int \alpha(x) dx = 1$, owing to kernel normalization), and also negative at high spatial frequencies, because $\tilde{\alpha}(\phi)$ approaches zero for large ϕ . However, if $\tilde{\alpha}(\phi)$ changes sign, so that it becomes negative for some intermediate frequency ϕ , $\lambda(\phi)$ can become positive. Third, when there is an Allee effect, for which $d'(N_0) < 0$, λ can become positive for intermediate frequencies even when $\tilde{\alpha}(\phi) \geq 0$ holds for all ϕ .

Results

To illustrate the influence of spatial processes on clustering along a gradient, we restrict ourselves to cases for which only a unimodal phenotypic distribution would appear in the absence of spatial effects: this applies when the competition kernel in trait space is wider than the carrying capacity density. For these situations our numerical analysis of equation (1) always found a

cline-like equilibrium solution of the form $n(u, x) = \eta(u - gx)$. By investigating the stability of this equilibrium, we have found two general destabilizing mechanisms. The first derives from competition kernels with shapes implying that their Fourier transform changes sign and the second from Allee effects. Both of these can lead to $\lambda(\phi) > 0$ for some spatial frequencies ϕ in equation (4).

KERNEL SHAPE

The influence of the shape of competition kernels is illustrated in Figures 1 and 2. As shown in Figure 1, box-like kernels have Fourier transforms with oscillating tails that include negative values. This property underlies the clustering in Figure 2A. Box-like kernels a_0 and a_1 cause competitive effects to stay relatively constant at small distances and then, beyond a characteristic distance, diminish rather rapidly. The resultant spacing between clusters depends on this characteristic distance, which is also related to the lowest spatial frequency (corresponding to the longest spatial scale) for which the Fourier transform of a kernel becomes negative. When the competition kernels instead have nonnegative Fourier transforms (and other factors causing clustering are absent), the stable equilibrium solution to equation (1) is a cline-like density, as illustrated in Figure 2B.

An intuitive explanation for the effect that box-like competition kernels promote clustering can be based on two observations. First, clusters with sufficiently large intercluster phenotypic and spatial distances will impose only weak competitive effects on each other. Second, when clusters are as close as possible without interfering much, an individual at a position intermediate between the clusters experiences the cumulative competitive effects originating from both adjacent clusters. Clustering is thus maintained because suitably spaced clusters largely escape competition from neighboring clusters, whereas “invaders” into positions intermediate between clusters suffer strong competitive effects from both neighboring clusters.

Because competition depends on distances in trait space and in geographical space, the phenotypic competition kernel a_0 and the spatial competition kernel a_1 can both influence clustering. The slope of the cline determines how traits and locations covary along the cline. Figure 3 shows aspects of the resulting pattern formation for different slopes g , using the same kernels as in Figure 2A. The overall effect is that clusters develop most rapidly for a slope at which the competitive effects described by the kernels a_0 and a_1 diminish in parallel along the cline, which happens for $g = 2$ in Figure 3A (for which $\sigma_0 = 2$ and $\sigma_1 = 1$). The spacing between clusters is determined by the kernel, either a_0 or a_1 , for which competitive effects drop off first along the cline. Along a cline with slope g , a given phenotypic increment is equal to g times the corresponding spatial increment. We should therefore expect the spatial intercluster distance p to be roughly proportional to the smallest of σ_1 and σ_0/g , that is,

$$p \propto \min(\sigma_1, \sigma_0/g), \quad (5)$$

where σ_0 and σ_1 are the widths of, respectively, the phenotypic and the spatial competition kernel and g is the slope of the cline. This prediction is corroborated by our numerical results: equation (5) with a factor of proportionality of about 2 gives an approximation to the intercluster distances in Figure 3B, and is in agreement with Figure 5 below.

It is also interesting to note that for very shallow clines (i.e., for values of g smaller than about 0.15 in Fig. 3), the phenotypic distributions of individual spatial clusters overlap considerably, so that the troughs between peaks become shallow: the trait distribution then displays only mild undulation, rather than strong clustering. This is illustrated by the mid-gap to peak ratio of the phenotypic density in Figure 3C. In the limit of g approaching zero, this undulation vanishes, and the mid-gap to peak ratio approaches 1 (left side of Fig. 3C). For steep slopes, clusters instead occur close together in geographical space, with the intercluster distance in trait space set by the shape of the kernel a_0 (right side of Fig. 3B). The perturbation growth rate becomes smaller for very steep slopes (right side of Fig. 3A) and clusters develop more slowly. This is the reason for the greater mid-gap to peak ratios for very steep slopes in Figure 3C. These curves are computed at time $t = 200$ after the introduction of the perturbation, and the dashed parts of the curves in Figure 3C indicate that an asymptotic equilibrium has not been reached by this time. By integrating equation (1) up to much greater values of t , we have found that phenotypic clusters eventually develop also for very steep slopes (not shown).

A steep slope of the environmental gradient leads to high mortality for locally adapted individuals that are displaced from positions near the cline. As a consequence, the maximum population density becomes low for steep slopes, which in turn reduces the importance of competition as a mortality-determining factor. This is likely to be the main reason for the smaller perturbation growth rate for steeper slopes in Figure 3A, illustrating the importance of competition for phenotypic pattern formation.

The basic reproduction ratio R_0 , defined as per capita birth rate divided by per capita death rate, can be used to illustrate how selection varies across trait values and spatial positions, and it can be helpful to view R_0 , as function of u and x , as a fitness landscape. For a clustered population, this fitness landscape could either be rather flat, with little variation in the per capita death rate, or there could be a substantial increase in the death rate for trait values and spatial positions intermediate between the clusters, resulting in a lower R_0 . In general, competition kernels that strongly promote clustering also give rise to a hilly fitness landscape for a clustered population. As shown in Figure 3C, the value of the basic reproduction ratio R_0 midway between clusters is about 55% of the value at the cluster centers for the situation with strongest

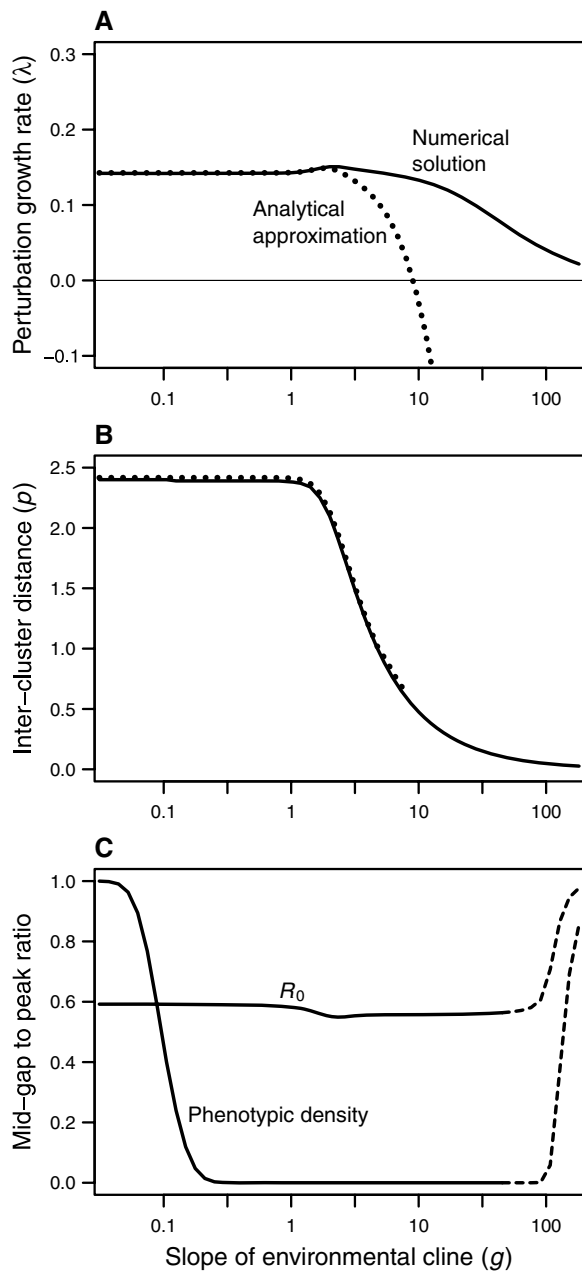


Figure 3. Effects of cline slope. Aspects of pattern formation, resulting from competition kernels having the 90% box-like shape illustrated in Figure 1, are presented as functions of the slope g of the environmental cline. Allee effects are absent. Numerical solutions are solutions to equation (1) and analytical approximations refer to the diffusion approximation given in equation (4). (A) The maximal exponential growth rate λ of perturbations of a cline-like equilibrium. For the numerical solution (solid curve), this rate was found by applying slight perturbations with different periods to a cline-like equilibrium density $n(u, x)$ and using a search algorithm to locate the largest λ (see text for further details). For the analytical approximation (dotted curve), equation (4) was used. (B) The intercluster distance given by the spatial period p at which the exponential growth rate λ is maximal, for the numerical solution (solid curve) and for the analytical approximation (partly

clustering ($g = 2$). This means that there will be persistent selection acting to maintain the clusters.

Results from the analytical approximation are also shown in Figure 3A, B. For shallow slopes, the approximation is rather accurate in determining the rate of perturbation growth, but for larger values of g , the approximated rate starts to deviate from the more accurate estimate obtained from the numerical solution. The reason is that mobility has a larger influence for steeper slopes; in an analysis using smaller values of σ_m , we found that the analytical approximation is accurate also for steeper slopes (not shown). When there is a deviation, the analytical approximation underestimates the potential for pattern formation (Fig. 3A), and can even fail qualitatively, by predicting stable cline-like solutions for steeper clines. Figure 4 illustrates the predictions obtained from the approximate analytical stability analysis of cline-like equilibria for a wider range of parameters.

The analytical approximation is useful in suggesting which qualitative factors are responsible for pattern formation. Examining equation (4), and assuming that there is no Allee effect ($d_0 = 0$), negative values of the transformed kernel $\tilde{\alpha}(\phi)$ are necessary for destabilizing the cline-like equilibrium. These negative values must be large enough and occur for spatial frequencies that are small enough not to be compensated by the counteracting influence of mobility, expressed by $m(2\pi\phi)^2$. For small spatial frequencies, the Fourier-transformed competition kernel will always be positive, because $\tilde{\alpha}(0) = \int \alpha(x)dx = 1$ holds owing to kernel normalization. For equation (1), this suggests that the shape of the effective competition kernel α along the environmental cline, that is, the shape of the product $a_0(gx)a_1(x)$, is important for the stability of a cline-like equilibrium. Our numerical investigations,

overlapping dotted curve, drawn for values of g for which the approximation indicates clustering). (C) Two different properties of clustered solutions to equation (1) at time $t = 200$ after slightly perturbing the cline-like equilibrium with a period that corresponds to the maximal λ . The dashed parts of the curves indicate that an asymptotic equilibrium has not been reached by this time. The curve labeled " R_0 " shows the value of R_0 for a trait value and spatial position midway between the cluster peaks relative to the value of R_0 at the cluster peaks, where R_0 is the basic reproduction ratio, defined as per capita birth rate divided by per capita death rate. A smaller mid-gap to peak ratio of R_0 corresponds to a more hilly fitness landscape for the clustered solution. The curve labeled "Phenotypic density" illustrates the degree of clustering in trait space: it shows the ratio between minimum and maximum density in trait space, while averaging over geographical space. A smaller mid-gap to peak ratio of the phenotypic density corresponds to a more hilly phenotypic distribution. Parameter values: $\sigma_K = 1$, $\sigma_0 = 2$, $\sigma_1 = 1$, $d_0 = 0$, $v_\mu = 0.01$, $\sigma_\mu = 0.05$, $v_m = 1$, and $\sigma_m = 0.05$.

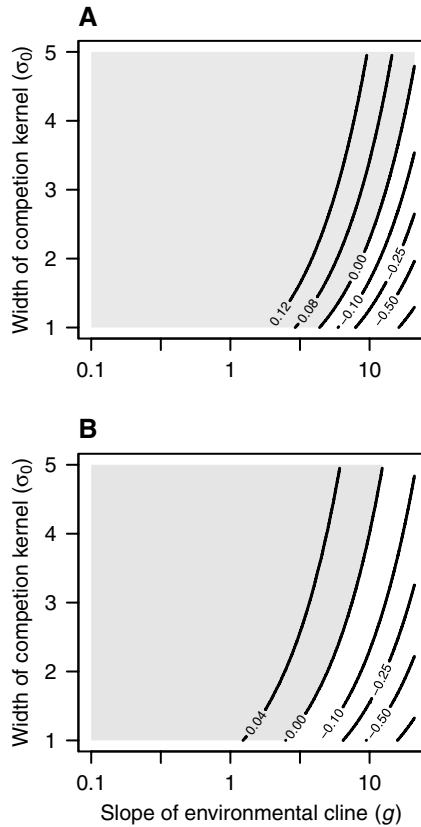


Figure 4. Analytical approximation. Based on equation (4), the maximal exponential growth rate λ of perturbations of the cline-like equilibrium is shown as a function of the slope g of the environmental cline and of the width σ_0 of the phenotypic competition kernel. The shape of the competition kernels is 90% box-like in (A) and 70% box-like in (B) (see Fig. 1 for illustrations of these kernels). Allee effects are absent. Shaded areas indicate parameter combinations for which $\lambda > 0$, which implies that the cline-like equilibrium is unstable. Parameter values: $m = 0.00125$, $\sigma_K = 1$, $\sigma_1 = 1$, and $d_0 = 0$.

beyond those reported in Figures 2 and 3, support this suggestion. In particular, we could numerically confirm the stability of cline-like equilibria for different competition kernels that make $\tilde{\alpha}(\phi)$ positive for all ϕ . These include (1) biexponential kernels, which have positive Fourier transforms (the transform of $\exp(-|x|)$ is $1/[1 + (2\pi\phi)^2]$), (2) kernels formed as the convolution of two kernels each of which has a positive Fourier transform, thus implying a positive Fourier transform of the convolution, as well as (3) kernels formed as the convolution of any symmetric kernel with itself, which results in nonnegative Fourier transforms. Even if one can find many examples of kernels with positive Fourier transforms (these are sometimes called positive definite kernels, in analogy with positive definite matrices), one should note that such kernels may be regarded as nongeneric. For an arbitrary symmetric, unimodal competition kernel, one ought to expect that its

Fourier transform becomes negative at certain frequencies, which, as we have seen above, can lead to clustering.

As a further illustration of the role played by the effective competition kernel along the cline (i.e., $\alpha(x) \propto a_0(gx)a_1(x)$), Figure 5 shows two cases of clustering. In the first case (Fig. 5A), the phenotypic competition kernel has a width such that, according to equation (5), it should determine intercluster distance ($\sigma_0 = 2$, $\sigma_1 = 1$, $g = 4$). The phenotypic kernel is box-like, whereas the spatial kernel is a Gaussian, so the phenotypic kernel both sets the scale of clustering and is the cause of clustering in Figure 5A. In Figure 5B, the phenotypic kernel is much wider ($\sigma_0 = 20$) and has Gaussian shape, but the spatial kernel is box-like, which implies that the spatial kernel both sets the scale of clustering and is the cause of clustering ($\sigma_1 = 1$, $g = 4$). In either of these cases, the effective competition kernel α along the cline is box-like, and it is helpful to regard the effect of the kernel α as a general form of frequency-dependent competition acting along the environmental cline. Figures 5A and 5B were obtained by starting the integration of equation (1) from a slightly perturbed cline-like equilibrium, which further demonstrates that the phenotypic and spatial competition kernels, acting in conjunction with the environmental cline, play very similar roles in phenotypic pattern formation.

ALLEE EFFECTS

Allee effects can cause pattern formation even when competition kernels are positive definite (e.g., when they have Gaussian shape). As can be seen in Figure 6A, the perturbation growth rate is greatest for clines of intermediate slope, and this phenomenon is more pronounced than the corresponding effect in Figure 3A.

There are several reasons why pattern formation is most promoted by environmental gradients of intermediate slope. In the analytical approximation in equation (4), the term $-N_0 d'(N_0)$ represents the Allee effect. With our assumptions for the Allee effect, this term exhibits a maximum for an intermediate value of N_0 . Because the value of N_0 increases with the slope g (because the normalizing factor C decreases with g), the Allee-effect term is largest for intermediate slopes. This phenomenon acts in combination with the Fourier transform $\tilde{\alpha}(\phi)$ of the competition kernel and with the effects of mobility to determine at which spatial frequency the maximum of λ occurs. When the competition kernel $\alpha(x)$ is broad, which will be the case for shallow slopes g , its Fourier transform $\tilde{\alpha}(\phi)$ is narrow, and therefore quickly approaches zero as ϕ increases. By contrast, a steep slope g causes $\alpha(x)$ to be narrow, which implies a broad Fourier transform $\tilde{\alpha}(\phi)$, which stays positive and large for a wider range of spatial frequencies. The net effect is that the perturbation growth rate is greatest for intermediate slopes (Fig. 6A). This effect is also seen in Figure 7, which, like Figure 4, illustrates the predictions obtained from the approximate stability analysis of cline-like equilibria for a wider range of parameters. That the growth rate λ is maximal

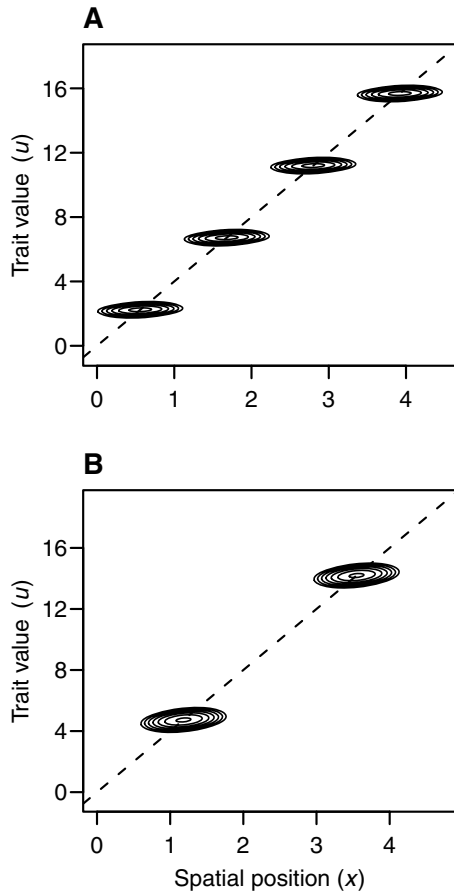


Figure 5. Stable equilibrium solutions. The contour plots show clustered densities $n(u,x)$ of solutions to equation (1) for different combinations of width and shape of the phenotypic and spatial competition kernels. In both depicted cases, the cline slope is $g = 4$. (A) The phenotypic competition kernel a_0 has width $\sigma_0 = 2$ and a 90% box-like shape, and the spatial competition kernel a_1 has width $\sigma_1 = 1$ and Gaussian shape. The intercluster distance, $\rho = 1.12$, is the spatial period for which there is maximal growth of perturbations of the cline-like equilibrium (the figure shows four periods of the pattern). According to equation (5), this period is set by the phenotypic competition kernel. The contour lines indicate density levels varying from 0.001 to 100 with even logarithmic spacing; the maximum density is 239.6. (B) The phenotypic competition kernel a_0 has width $\sigma_0 = 20$ and Gaussian shape, and the spatial competition kernel a_1 has width $\sigma_1 = 1$ and a 90% box-like shape. The intercluster distance, $\rho = 2.365$, is the spatial period for which there is maximal growth of perturbations of the cline-like equilibrium (the figure shows two periods of the pattern). According to equation (5), this period is set by the spatial competition kernel. The contour lines indicate density levels varying from 0.001 to 1000 with even logarithmic spacing and the maximum density is 1530. Both panels show the clustered pattern at time $t = 1000$, when the density is close to a stable equilibrium. The initial density at time $t = 0$ was given by an oscillating perturbation ($\epsilon = 0.001$) of a cline-like equilibrium solution. Other parameter values: $\sigma_K = 1$, $d_0 = 0$, $\nu_\mu = 0.01$, $\sigma_\mu = 0.05$, $\nu_m = 1$, and $\sigma_m = 0.05$.

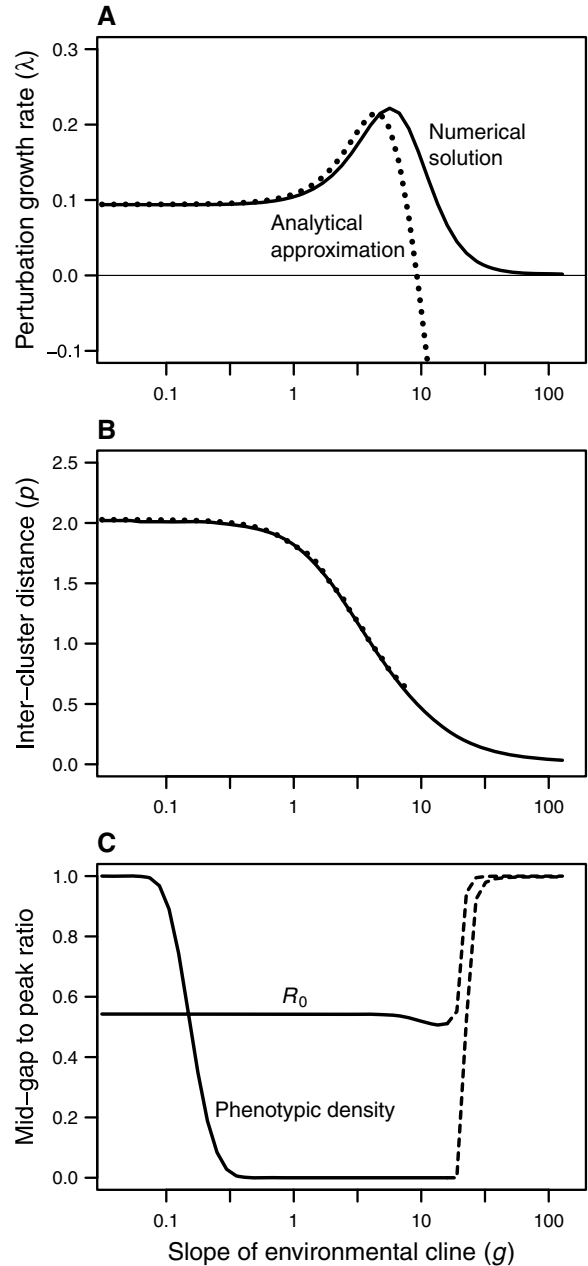


Figure 6. Effects of cline slope. Aspects of pattern formation resulting from an Allee effect with $d_0 = 0.8$ and $n_0 = 10$, for Gaussian competition kernels, presented as functions of the slope g of the environmental cline. Panels (A)–(C) show the same quantities as the corresponding panels in Figure 3. Parameter values: $\sigma_K = 1$, $\sigma_0 = 2$, $\sigma_1 = 1$, $\nu_\mu = 0.01$, $\sigma_\mu = 0.05$, $\nu_m = 1$, and $\sigma_m = 0.05$.

at intermediate slopes is particularly evident in Figure 7A, where the Allee effect is more pronounced.

Just as for competition kernels that are not positive definite (Fig. 3A), the growth rate of perturbations can be positive for very shallow slopes (left side of Fig. 6A), resulting in geographical clusters with considerable phenotypic overlap (left side of Fig. 6C).

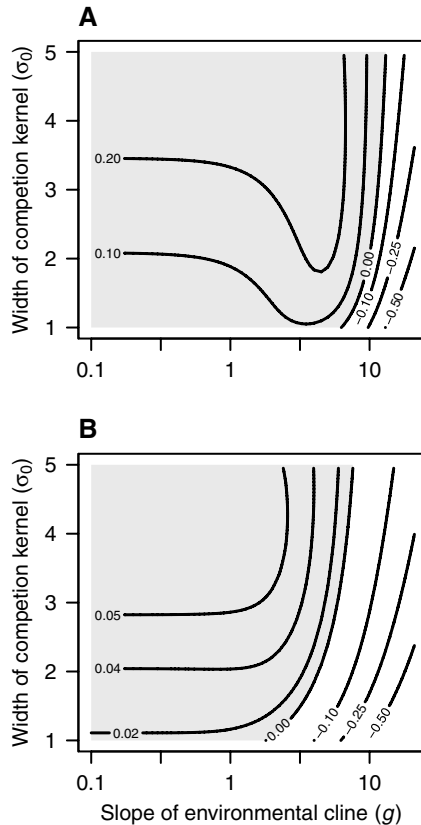


Figure 7. Analytical approximation. The maximal exponential growth rate λ of perturbations of the cline-like equilibrium is presented in the same way as in Figure 4. There is an Allee effect with $d_0 = 0.8$ and $n_0 = 10$ in (A) and with $d_0 = 0.2$ and $n_0 = 10$ in (B). The competition kernels are Gaussians.

For very steep slopes g , the perturbation growth rate approaches zero (right side of Fig. 6A), implying that clusters develop very slowly. The explanation is that the influence of mobility is stronger for steeper slopes, reducing maximum population density and thus also reducing the relative importance of an Allee effect.

The decrease in intercluster distances for larger values of the slope, as shown in Figure 6B, is similar to that seen in Figure 3B. The explanation is also similar: the spacing between the fastest growing clusters is determined by the competition kernel, either a_0 or a_1 , for which competitive effects drop off first along the cline. This is expressed by equation (5), which applies both to Figure 3B and to Figure 6B, demonstrating that competition plays an important role in cluster formation also when an Allee effect is responsible for destabilizing the cline-like equilibrium.

Just as for clustering caused by kernel shapes, the Allee effect can produce fitness landscapes for clustered populations that are rather hilly (Fig. 6C). Note that, if the distribution in geographical space is sharply clustered, the excess per capita rate of mortality caused by the Allee effect midway between the clusters, compared to the peaks, can be at most d_0 . Finally, our analysis shows that

weak Allee effects can cause phenotypic pattern formation. Strong Allee effects, which correspond to $d_0 > 1$ in our model, would have an even stronger destabilizing effect on a cline-like equilibrium, but we have not investigated their influence further.

EFFECTS OF MOBILITY

In our model, movement-based gene flow and mutation are the main factors countering pattern formation. Mobility will smooth out density variation over small distances and, because individuals become displaced from positions near the cline, mobility can also increase overall mortality, in effect making competition less important as a mortality-determining factor.

Although our analytical approximation in equation (4) predicts a maximum mobility for which a cline-like equilibrium can be destabilized (this maximum corresponds to a σ_m of up to around 0.1 to 0.2 for the parameter ranges in Figures 4 and 7), the approximation underestimates the potential for clustering of solutions to equation (1). This is demonstrated in Figure 8, which shows examples of clustering with higher mobility. Even though the strength of selection maintaining the clustered state is weaker than it would be for less mobility, it is still noticeable: for Figures 8A and 8B, respectively, the basic reproduction ratio R_0 midway between the clusters is 60% and 73% of its value at the peaks.

From our numerical analysis of equation (1), we have found that greater mobility slows down the rate of phenotypic pattern formation. This phenomenon is analogous to the smaller perturbation growth rate for steep slopes g in Figures 3A and 6A. Sufficiently high mobility can also prevent pattern formation. For instance, using parameter values as in Figure 8B, we could numerically establish that the cline-like equilibrium was stable when mobility was increased to $\sigma_m = 0.4$.

We have also found that the stabilizing influence of mobility becomes stronger if mobility is combined with a high rate of mutation. The reason is that when these processes act together, density differences along the cline $u = gx$ are equalized more easily. For instance, a consequence of mobility in Figure 8 is a broadening of the density distribution in the spatial direction, but movement of individuals does not by itself smooth out density variation along the cline. Similarly, mutation does not by itself smooth out density variation along the cline; a combination of movement and mutation is needed for this. Mobility combined with a very high rate of mutation thus has the potential to prevent pattern formation along an environmental gradient, although the required rate of mutation might not be realistic.

Discussion

Our analysis confirms the basic contention of Doebeli and Dieckmann (2003) that gradual spatial variation in environmental conditions, affecting selection on a quantitative trait, can lead to essentially discrete variation in the evolved trait. Our results

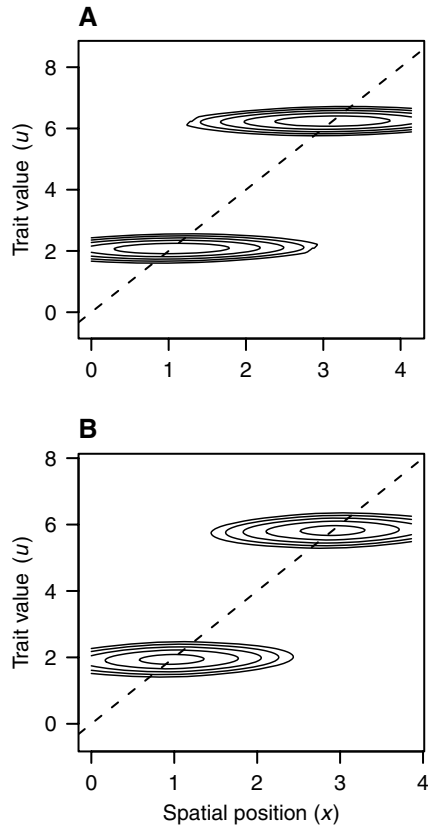


Figure 8. Stable equilibrium solutions. The contour plots show clustered densities $n(u,x)$ of solutions to equation (1) for cases with higher mobility. (A) Competition kernels have a 90% box-like shape. The increased movement distance $\sigma_m = 0.5$, in conjunction with the mobility rate $\nu_m = 1$, leads to less-pronounced clustering compared with Figure 2A. The contour lines indicate density levels varying from 0.001 to 10 with even logarithmic spacing; the maximum density is 59.1. (B) Competition kernels are Gaussian, but there is an Allee effect with $d_0 = 0.8$ and $n_0 = 10$, and the mobility parameters are $\nu_m = 1$ and $\sigma_m = 0.2$. The contour lines indicate density levels varying from 0.001 to 10 with even logarithmic spacing; the maximum density is 25.4. Both panels show two whole periods of the clustered pattern at time $t = 1000$, when the density is close to a stable equilibrium. The initial density at time $t = 0$ was given by an oscillating perturbation ($\varepsilon = 0.1$) of the cline-like equilibrium solution. Other parameter values: $g = 2$, $\sigma_K = 1$, $\sigma_0 = 2$, $\sigma_1 = 1$, $\nu_\mu = 0.01$, and $\sigma_\mu = 0.05$.

are also in accordance with their suggestion that gradients of intermediate slope are most prone to cause clustering of the trait distribution, because we find that these gradients lead to faster growth of perturbations of a cline-like equilibrium solution. It is important to note that, because of the interplay of local competition and local adaptation, cluster formation along environmental gradients can occur even when frequency-dependent competition would not give rise to clustering in spatially unstructured, well-mixed populations. Our analysis shows that under these conditions, phenotypic pattern formation is possible for environmental

gradients with slopes ranging from rather shallow to quite steep.

The main novel contribution of our work is a richer understanding of how the shape of competition kernels influences pattern formation. Competition kernels have been used extensively in ecology and evolution as a means of representing variation in the strength of competition with phenotypic or spatial distance, with application to questions such as species packing, character displacement, phenotypic and spatial clustering, and speciation (e.g., MacArthur 1972; Roughgarden 1972, 1979; May 1973; Slatkin 1979, 1980; Bulmer 1980; Sasaki 1997; Kirkpatrick and Barton 1997; Dieckmann and Doebeli 1999; Case and Taper 2000; Doebeli and Dieckmann 2003). In spite of the very wide use of competition kernels in modeling, our work and the analysis by Pigolotti et al. (2007) are the first to provide a general analysis of the effects of kernel shape, using the Fourier transform of a kernel. The insights gained from these analyses are likely to have an impact on other problem areas where competition kernels are used in modeling.

It might at first seem surprising that continuous and gradual variation in environmental conditions could produce a discrete evolutionary response. Yet, there are many other examples of continuity giving rise to discreteness, for instance evolutionarily stable strategies in fluctuating environments (Sasaki and Ellner 1995) or life-history responses to size-selective mortality (Taborsky et al. 2003), so this is not an exceptional phenomenon. In fact, extending earlier work by Sasaki and Ellner (1995) and Sasaki (1997), Gyllenberg and Mesz ena (2005) proved that coexistence of a continuum of strategies under competition is a nongeneric outcome. Instead, in the absence of mutation and movement, the typical evolutionary outcome under frequency-dependent competition is a discrete trait distribution. This is an important insight, but more can be said about the matter. Even if selection generically acts to produce discreteness in trait distributions, its strength could vary from case to case. The strength of selection is of particular importance when counteracting forces tend to smooth out a distribution. This may occur through mutation and, as in our model here, through movement-based gene flow between nearby locations.

Deterministic models with Gaussian competition kernels are well known to allow continuous equilibrium distributions (Roughgarden 1979). These models can be regarded as degenerate and structurally unstable (Gyllenberg and Mesz ena 2005), at least when one ignores the smoothing influences of mutation and gene flow. In analyzing our deterministic model we found a much wider class of kernels, namely those with positive Fourier transforms, that lead to continuous equilibrium distributions also in the limit of no mutation and no gene flow. When such a kernel is slightly perturbed, so as to lose its property of positive definiteness, one should expect selection toward clustering to appear, indicating a possible structural instability of the continuous equilibrium distribution, but the strength of this selection may be rather weak

(a similar argument was made for optimal strategies in fluctuating environments; Haccou and Iwasa 1998). From the insight gained in our analysis here, perturbing a kernel that has a positive Fourier transform should typically result in a transform that changes sign. Such sign changes are likely to occur at high phenotypic or spatial frequencies, where the transform of the unperturbed kernel is close to zero; accordingly, the perturbed kernel will select for a discrete distribution consisting of closely spaced morphs. This implies, in turn, that counteracting forces like mutation and movement are particularly efficient at smoothing out such distributions, thus giving a certain structural robustness to the unperturbed equilibrium.

Although the strength of selection toward clustering can sometimes be weak, as was argued by Polechová and Barton (2005), our analysis showed that in other cases it can be quite substantial, with a correspondingly hilly fitness landscape for populations close to a clustered equilibrium. We have demonstrated that competition kernels with box-like shapes, as well as Allee effects, can render clustering rather resistant to counteracting forces. Such cases are also characterized by clustering evolving more rapidly from a nonclustered initial state.

Doebeli and Dieckmann (2003) used Gaussian competition kernels, which means that competition in trait space and geographical space acted together with one or several other processes in contributing to the clustering observed in their analysis. For instance, effects inherent to finite populations of discrete individuals will have contributed to the observed clustering. It has been known for some time that individual-based models of populations in continuous space show local clumping of individuals, beyond what is expected from a Poisson distribution, because of reproductive pair correlations (Felsenstein 1975; Bolker and Pacala 1997; Young et al. 2001; Law et al. 2003). Similar processes will also operate in the trait space of a continuous character changing through local mutation. With competition along an environmental gradient influencing the phenotypic and spatial scales of fluctuations, the outcome can be a clustering of phenotypes. The phenomenon is a consequence of the discreteness of individuals, which, of course, corresponds to the real situation in nature. Unfortunately, approximate deterministic formulations like reaction–diffusion models do not account for this. It can be shown (U. Dieckmann, unpubl. data) that accounting for finite population size in reaction–diffusion models results in corrections that are similar to an Allee effect, even for asexual populations. For sexual populations, a traditionally acknowledged Allee effect results from the decrease of fecundity when suitable mates are locally rare. This effect was accounted for in the analysis of sexual populations by Doebeli and Dieckmann (2003), and will thus have contributed to clustering in those cases.

To demonstrate the effects of spatial structure as clearly as possible, our analysis here has focused on cases in which stabiliz-

ing selection is stronger than the disruptive effect of competition in trait space. Situations in which, instead, the disruptive effects are stronger than stabilizing effects are also of interest. In our model, these situations arise whenever the carrying capacity density is wider than the competition kernel ($\sigma_K > \sigma_0$). Under these circumstances, phenotypic clusters can be expected to coexist locally. Some of the factors we have dealt with, like the shape of competition kernels, are likely to be of importance also for such local cluster formation (but our approximate analytical treatment does not extend to these situations). For sexual populations, local coexistence raises interesting questions about the degree of reproductive isolation between clusters. Because of gene flow between spatially segregated, but adjacent clusters, such questions are also relevant for the ecological situations we have dealt with here ($\sigma_K < \sigma_0$), although they may be less urgent. Although assortative mating is often viewed as a mechanism to reduce gene flow between clusters, the role of frequency-dependent competition in local cluster formation has recently been questioned (Polechová and Barton 2005). We have shown elsewhere that frequency-dependent competition and assortative mating can promote cluster formation in a well-mixed sexual population, even for the case of Gaussian competition kernels (Doebeli et al. 2007). Assortative mating can therefore be expected also to promote cluster formation along an environmental gradient, as in the individual-based sexual models of Doebeli and Dieckmann (2003).

Our analysis involved a search for cline-periodic solutions. These solutions presume an infinitely extended spatial domain and the main motivation for studying them is that they help disentangle nonboundary effects from possible boundary effects. Results obtained in this way are relevant for spatial domains that are large compared to the spatial period of phenotypic clustering, in particular for the part of the domain that is far away from the boundary. Because phenomena in nature necessarily occur in finite geographical domains, it is important also to consider the influence of boundaries. Effects of boundaries on phenotypic clustering are real biological phenomena, worthy of study, and not to be dismissed as artifacts. It is helpful to distinguish two types of boundary effects. First, if the carrying capacity decreases toward the limits of a spatial region but there is no barrier to dispersal across the boundary, one may expect low population density near the boundary and a phenotypic cluster some distance away from the boundary. Second, if instead the boundary is a barrier to dispersal, there may be a phenotypic cluster located at or very near the boundary. Although a boundary of the latter type was included in the analysis by Doebeli and Dieckmann (2003), our results here have demonstrated that boundary effects by no means are required for phenotypic pattern formation.

We found a striking similarity in the effects of phenotypic and spatial competition kernels. As seen, for instance, in Figure 5,

either kernel can give rise to clustering. An intuitive explanation for this similarity in effects is that local adaptation in a population distributed along an environmental gradient produces a correlation between phenotype and spatial position (Doebeli and Dieckmann 2003). This means that variation in the strength of competition with spatial distance in effect becomes variation in the strength of competition with phenotypic distance. Interpreted in a broad sense, both the effects of the phenotypic competition kernel and the spatial competition kernel, acting along an environmental gradient, are instances of frequency-dependent competition.

A general conclusion from our analysis is that local frequency-dependent competition, interpreted in a broad sense, plays a crucial role in phenotypic pattern formation, even when additional processes, like Allee effects, are required for clustering to occur. The influence of competition is evident in the dependence of intercluster distances on the combined characteristics of the cline and the phenotypic and spatial competition kernels. The dependence is described by equation (5) and applies to all our analyses of clustering here. This kind of relationship will be a general feature of phenotypic pattern formation induced by competition along environmental gradients, and could therefore help understand patterns in real populations. If phenotypic clustering is driven by competition, intercluster distances will reflect the scale of competitive influence along a cline, in the sense that competitive effects between clusters have diminished at the intercluster distance, but would increase for considerably smaller distances, thus preventing the growth of intermediate clusters.

For environmental gradients with shallow slopes, we found that spatial clusters may evolve, but, because of phenotypic overlap, this would not entail phenotypic pattern formation. We also found that steep slopes could give rise to phenotypic clusters, but the process is quite slow, leaving intermediate slopes as the most favorable setting for phenotypic pattern formation. In presenting our results, we used the width of the spatial competition kernel as spatial unit (by setting $\sigma_1 = 1$) and the width of the carrying capacity as phenotypic unit (by setting $\sigma_K = 1$); it is thus relative to these units that we ought to interpret a gradient's slope as being shallow, intermediate, or steep. For instance, a shallow slope is one for which the locally best-adapted phenotype changes little over the distance measured by the width of the spatial competition kernel, and an intermediate slope corresponds to a spatial range of competitive effects over which there is a noticeable, but not very large, change in the locally best-adapted phenotype. When assessing the spatial range of competition in real populations, it is worth noting that there are several processes that can increase this range, for instance, greater mobility in foraging than in reproductive dispersal, as well as mobility in a prey resource that individuals compete for. So-called apparent competition (Holt 1977; Holt and Lawton 1994), resulting from local populations sharing mobile predators or parasites (Morris et al. 2005), is another general

mechanism that can extend the range of competitive influences.

Because we made several assumptions in our analysis (for instance, that local population sizes are large and that stabilizing selection is stronger than the disruptive effect of competition in trait space), it is important to note that there are further causes of phenotypic clustering beyond those of competition kernel shape and Allee effects that we have studied here. Overall, the range of ecological situations promoting phenotypic clustering along environmental gradients is likely to be broad.

ACKNOWLEDGMENTS

We thank N. Barton and two anonymous referees for helpful comments. This work was supported by a grant from the Swedish Research Council to OL. MD acknowledges the support of the James S. McDonnell Foundation (USA) and of NSERC (Canada). UD acknowledges financial support by the Vienna Science and Technology Fund, WWTF.

LITERATURE CITED

- Barton, N. H. 1999. Clines in polygenic traits. *Genet. Res.* 74:223–236.
- Bazykin, A. D. 1969. Hypothetical mechanism of speciation. *Evolution* 23:685–687.
- Bolker, B., and S. W. Pacala. 1997. Using moment equations to understand stochastically driven spatial pattern formation in ecological systems. *Theor. Pop. Biol.* 52:179–197.
- Bulmer, M. G. 1980. *The mathematical theory of quantitative genetics*. Clarendon Press, Oxford, U. K..
- Case, T. J., and M. L. Taper. 2000. Interspecific competition, environmental gradients, gene flow, and the coevolution of species' borders. *Am. Nat.* 155:583–605.
- Dieckmann, U., and M. Doebeli. 1999. On the origin of species by sympatric speciation. *Nature* 400:354–357.
- Doebeli, M., and U. Dieckmann. 2003. Speciation along environmental gradients. *Nature* 421:259–264.
- . 2004. Adaptive dynamics of speciation: spatial structure. Pp. 140–167 in U. Dieckmann, J. A. J. Metz, M. Doebeli, and D. Tautz, eds. *Adaptive speciation*. Cambridge Univ. Press, Cambridge.
- Doebeli, M., H. J. Blok, O. Leimar, and U. Dieckmann. 2007. Multimodal pattern formation in phenotype distributions of sexual populations. *Proc. R. Soc. Lond. B* 274:347–357.
- Endler, J. A. 1977. *Geographic variation, speciation, and clines*. Princeton Univ. Press, Princeton, NJ.
- Felsenstein, J. 1975. A pain in the torus: some difficulties with models of isolation by distance. *Am. Nat.* 109:359–368.
- Fisher, R. A. 1950. Gene frequencies in a cline determined by selection and diffusion. *Biometrics* 6:353–361.
- Geritz, S. A. H., É. Kisdi, G. Meszéna, and J. A. J. Metz. 1998. Evolutionarily singular strategies and the adaptive growth and branching of the evolutionary tree. *Evol. Ecol.* 12:35–57.
- Gyllenberg, M., and G. Meszéna. 2005. On the impossibility of coexistence of infinitely many strategies. *J. Math. Biol.* 50:133–160.
- Gyllenberg, M., J. Hemminki, and T. Tammaru. 1999. Allee effects can both conserve and create spatial heterogeneity in population densities. *Theor. Pop. Biol.* 56:231–242.
- Haccou, P., and Y. Iwasa. 1998. Robustness of optimal mixed strategies. *J. Math. Biol.* 36:485–496.
- Haldane, J. B. S. 1948. The theory of a cline. *J. Genet.* 48:277–284.
- Holt, R. D. 1977. Predation, apparent competition and the structure of prey communities. *Theor. Pop. Biol.* 12:197–229.

- Holt, R. D., and J. H. Lawton. 1994. The ecological consequences of shared natural enemies. *Ann. Rev. Ecol. Syst.* 25:495–520.
- Hopf, F. A., and F. W. Hopf. 1985. The role of the Allee effect in species packing. *Theor. Pop. Biol.* 27:27–50.
- Keitt, T. H., M. A. Lewis, and R. D. Holt. 2001. Allee effects, invasion pinnings and species' borders. *Am. Nat.* 157:203–216.
- Kirkpatrick, M., and N. H. Barton. 1997. Evolution of a species' range. *Am. Nat.* 150:1–23.
- Law, R., D. J. Murrell, and U. Dieckmann. 2003. Population growth in space and time: spatial logistic equations. *Ecology* 84:252–262.
- MacArthur, R. H. 1972. *Geographical ecology: patterns in the distribution of species.* Harper and Row, New York.
- May, R. M. 1973. *Stability and complexity in model ecosystems.* Princeton Univ. Press, Princeton, NJ.
- Metz, J. A. J., R. M. Nisbet, and S. A. H. Geritz. 1992. How should we define fitness for general ecological scenarios? *Trends Ecol. Evol.* 7:198–202.
- Metz, J. A. J., S. A. H. Geritz, G. Meszéná, F. J. A. Jacobs, and J. S. van Heerwaarden. 1996. Adaptive dynamics, a geometrical study of nearly faithful reproduction. Pp. 183–231 in S. J. van Strien and S. M. Verduyn Lunel, eds. *Stochastic and spatial structures of dynamical systems. Proceedings of the Royal Dutch Academy of Science (KNAW Verhandelungen).* North-Holland, Amsterdam.
- Morris, R. J., O. T. Lewis, and H. C. J. Godfray. 2005. Apparent competition and insect community structure: towards a spatial perspective. *Ann. Zool. Fenn.* 42:449–462.
- Okubo, A., A. Hastings, and T. Powell. 2001. Population dynamics in temporal and spatial domains. Pp. 298–373 in A. Okubo and S. A. Levin, eds. *Diffusion and ecological problems, 2nd ed.* Springer, New York.
- Pigolotti, S., C. López, and E. Hernández-García. 2007. Species clustering in competitive Lotka-Volterra models. *Phys. Rev. Lett.* 98:258101.
- Polechová, J., and N. H. Barton. 2005. Speciation through competition: a critical review. *Evolution* 59:1194–1210.
- Press, W. H., S. A. Teukolsky, W. T. Vetterling, and B. P. Flannery. 1992. *Numerical recipes in C: the art of scientific computing, 2nd ed.* Cambridge Univ. Press, Cambridge.
- Roughgarden, J. 1972. The evolution of niche width. *Am. Nat.* 106:683–718.
- . 1979. *Theory of population genetics and evolutionary ecology: an introduction.* Macmillan, New York.
- Sasaki, A. 1997. Clumped distribution by neighborhood competition. *J. Theor. Biol.* 186:415–430.
- Sasaki, A., and S. Ellner. 1995. The evolutionarily stable phenotype distribution in a random environment. *Evolution* 40:337–350.
- Slatkin, M. 1978. Spatial patterns in the distribution of polygenic characters. *J. Theor. Biol.* 70:213–228.
- . 1979. Frequency- and density-dependent selection on a quantitative character. *Genetics* 93:755–771.
- . 1980. Ecological character displacement. *Ecology* 61:163–177.
- Taborsky, B., U. Dieckmann, and M. Heino. 2003. Unexpected discontinuities in life-history evolution under size-dependent mortality. *Proc. R. Soc. Lond. B* 270:713–721.
- Taylor, C. M. and A. Hastings. 2005. Allee effects in biological invasions. *Ecol. Lett.* 8:895–908.
- Turing, A. M. 1952. The chemical basis of morphogenesis. *Philos. Trans. R. Soc. Lond. B* 237:37–72.
- Wang, M. H. and M. Kot. 2001. Speeds of invasion in a model with strong or weak Allee effects. *Math. Biosci.* 171:83–97.
- Young, W. R., A. J. Roberts, and G. Stuhne. 2001. Reproductive pair correlations and the clustering of organisms. *Nature* 412:328–331.

Associate Editor: M. Van Baalen

APPENDIX

Here we give a brief description of the numerical procedures used to analyze equation (1), followed by derivations relating to the approximate analytical treatment in equations (2)–(4).

NUMERICAL ANALYSIS

In applying our approach, we need to find cline-like equilibrium solutions $\eta(u - gx)$ also in situations for which the cline-like equilibrium is unstable for certain periods p . This can be achieved by looking for equilibrium solutions that have sufficiently short period p . When imposing cline periodicity with a sufficiently small period p , our numerical approach always found a cline-like equilibrium solution. This solution is of course a cline-periodic equilibrium for any period p . Having identified a cline-like equilibrium $\eta(u - gx)$, we investigated its stability for a given period p by integrating equation (1), starting at $t = 0$ with the perturbed, cline-periodic equilibrium density

$$n(u, x, 0) = [1 - \varepsilon \cos(2\pi x/p)]\eta(u - gx),$$

typically using a small amplitude $\varepsilon = 0.001$ of perturbation. For small deviations from the equilibrium, equation (1) is approximately linear in the deviation $\psi(u, x, t) = n(u, x, t) - \eta(u - gx)$ and can thus be analyzed as an eigenvalue problem, provided there are solutions of the form $\psi(u, x, t) = \rho(u, x) \exp(\lambda t)$. We did not directly use this approach, but instead assumed that the deviation approached such a form. The parameter λ then takes the role of the dominant eigenvalue and can be estimated as the maximal growth rate of the deviation using numerical solutions of equation (1). A positive λ implies instability of the cline-like equilibrium and for these cases we studied the formation of clusters by integrating equation (1) over a longer time interval (we report results on the characteristics of clustering at time $t = 200$ after the introduction of the small perturbation).

We used the rectangle (midpoint) rule to compute the integrals needed for the right-hand side of equation (1) and Euler's method with a suitably small time step Δt to integrate forward in time. To conveniently impose cline periodicity with spatial period p for a given slope g of the cline, we selected grid spacings Δu and Δx in trait space and geographical space such that the periods gp and p in these spaces were multiples of the corresponding grid spacing. We verified the numerical accuracy of our solutions by checking that essentially the same solution was obtained when recomputing with halved spacings. We also made sure that the range of integration in trait space was wide enough to accurately capture the effects of mobility. Movements in geographical space produce deviations from the cline $u = gx$, so that the range of integration in trait space needs to be wider for steeper slopes g . As an example, for the solutions depicted in Figure 2 we used

$\Delta u = 0.02$, $\Delta x = 0.01$, $\Delta t = 0.05$, and a range of integration in trait space from $gx - 8$ to $gx + 8$.

For a given slope g , we first computed a cline-like solution $\eta(u - gx)$ by imposing a short period p_0 and integrating equation (1) numerically over a sufficient time interval to approach an equilibrium (we used a time interval of duration 400). With small enough p_0 , our method always found such a cline-like equilibrium. To be able to extend this solution to a longer period p , the period p_0 was chosen as a multiple of the grid spacing Δx .

To estimate, for a given period p , the rate of steady exponential growth of a perturbation of the cline-like equilibrium, we used the density $n(u, x)$ and its time derivative $\partial n(u, x)/\partial t$ along the cline $u = gx$. Each of these defines a one-dimensional periodic function, and we computed the (complex) Fourier component of each of these functions at the spatial frequency $1/p$. We then estimated λ as the best-fitting real coefficient of proportionality between the two Fourier components. To minimize the contribution to the estimated growth rate λ of other eigenmodes with $\lambda' < \lambda$, we performed this computation at a time t that was as long as possible after the introduction of the perturbation at $t = 0$, but before a growing perturbation became big enough to involve nonlinear effects or a decaying perturbation became too small to be resolved numerically. When this approach produced a positive λ , we continued the integration of equation (1) up to a time $t = 200$ after the introduction of the perturbation. This always produced a clustered solution, thus validating our approach to estimating the stability of the cline-like equilibrium.

For a given set of parameters, including the slope g , we repeated the above procedure for different periods p , systematically searching (using golden section search) for the period having the highest perturbation growth rate λ . The entire numerical procedure was implemented as a C++ program.

APPROXIMATE ANALYTICAL TREATMENT

When searching for cline-like solutions of the form $\eta(u - gx)$, which are functions of the deviation $z = u - gx$ of the trait u from the local maximum of the carrying capacity at gx , it is convenient to introduce this deviation as a variable in equation (1). Considering the limit of small σ_μ^2 and σ_m^2 (see, e.g., Doebeli and Dieckmann 2004), and introducing the diffusion coefficients

$$\mu = \frac{1}{2}v_\mu\sigma_\mu^2, m = \frac{1}{2}v_m\sigma_m^2,$$

equation (1) is transformed into a reaction–diffusion equation

$$\begin{aligned} \frac{\partial}{\partial t} n(z, x) = & [1 - n_c(z, x)/\kappa(z) - d(\bar{n}(x))] n(z, x) \\ & + \left[(\mu + mg^2) \frac{\partial^2}{\partial z^2} - 2mg \frac{\partial^2}{\partial z \partial x} + m \frac{\partial^2}{\partial x^2} \right] n(z, x). \end{aligned} \quad (\text{A1})$$

For a cline-like density $\eta(z)$ one finds, by integrating over the spatial coordinate, an effective competition kernel for the deviation z given by

$$\alpha_0(z) = \int a_0(z + gx)a_1(x)dx,$$

and a corresponding effective density

$$\eta_c(z) = \int \alpha_0(z' - z)\eta(z')dz'.$$

Equation (A1) for a cline-like equilibrium density $\eta(z)$ then becomes

$$\frac{\partial}{\partial t} \eta(z) = 0 = [1 - \eta_c(z)/\kappa(z) - d(\bar{\eta})]\eta(z) + (\mu + mg^2) \frac{\partial^2}{\partial z^2} \eta(z). \quad (\text{A2})$$

In the limit of small μ and m we expect solutions for which the equilibrium density is concentrated around $z = 0$, so it is of interest to expand the effective competition kernel for small z ,

$$\alpha_0(z) \approx C \left(1 - \frac{1}{2}z^2/s_0^2\right),$$

where

$$C = \alpha_0(0) = \int a_0(gx)a_1(x)dx$$

is a normalization constant. We can introduce the ansatz from equation (2) into equation (A2) and identify terms. The lowest-order coefficient N_0 in equation (2) must satisfy

$$N_0C + d(N_0) = 1.$$

This is because N_0C is the per capita death rate from competition and $d(N_0)$ is the per capita death rate from the Allee effect, for a density of the form $N_0\delta(u - gx)$. At equilibrium these rates must balance the per capita birth rate of 1. Our assumptions for the Allee effect imply that there is a unique solution for N_0 , which will be positive. For σ^2 we obtain to lowest nonvanishing order

$$\sigma^2 = \sqrt{\frac{2(\mu + mg^2)s_0^2\sigma_K^2}{N_0C(s_0^2 - \sigma_K^2)}}.$$

For this expression to be meaningful, we must assume $\sigma_K^2 < s_0^2$, which is a requirement for stabilizing selection to be stronger than the locally diversifying effect of competition. Note also that σ^2 goes to zero as μ and m go to zero, but that this approach is relatively slow, in particular for large g . Finally, there is an expression

$$N_1 = \frac{N_0C}{C + d'(N_0)} \left(\frac{1}{s_0^2} - \frac{1}{2\sigma_K^2} \right)$$

for the parameter N_1 in equation (2).

To study the dynamics of perturbations of a cline-like equilibrium, we can introduce the ansatz from equation (3) into equation

(A1), making the assumption of a small $w(x)$ and introducing the expressions for N_0 , N_1 , and σ^2 from the preceding paragraph. Using the competition kernel

$$\alpha(x) = \frac{1}{C} a_0(gx) a_1(x),$$

we obtain an approximate reaction–diffusion equation for $w(x)$,

$$\begin{aligned} \frac{\partial}{\partial t} w(x) = & -N_0 C \int \alpha(x' - x) w(x') g x' - N_0 d'(N_0) w(x) \\ & + m \frac{\partial^2}{\partial x^2} w(x), \end{aligned} \quad (\text{A3})$$

where d' is the derivative of the Allee effect function. This equation describes how competition, the Allee effect, and mobility affect the deviation from a cline-like equilibrium. A relationship including only terms representing the lowest nonvanishing order in m is obtained by removing the last term in equation (A3), because this term is proportional to m . From our numerical analysis, we have found that inclusion of the last term improves the approximation for values of m that are small enough to make the term small. Conversely, if the spatial variation in w is rapid enough to make

the term dominate the right-hand side of equation (A3), we have found that the approximation is no longer accurate.

Because equation (A3) is linear in w and involves a convolution of w with the kernel α , it is helpful to Fourier transform it. Defining the Fourier transform of a function $f(x)$ as

$$\tilde{f}(\phi) = \int f(x) \exp(-i2\pi\phi x) dx,$$

where ϕ is a spatial frequency and i is the imaginary unit, we obtain the Fourier transform of equation (A3) as

$$\frac{\partial}{\partial t} \tilde{w}(\phi) = -N_0 C \tilde{\alpha}(\phi) \tilde{w}(\phi) - N_0 d'(N_0) \tilde{w}(\phi) - m(2\pi\phi)^2 \tilde{w}(\phi). \quad (\text{A4})$$

If $w(x)$ is periodic with period p , the transform $\tilde{w}(\phi)$ will be a sum of delta peaks located at spatial frequencies that are multiples of $1/p$. Making the ansatz $\tilde{w}(\phi', t) = \delta(\phi' - \phi) \exp[\lambda(\phi)t]$, we see that a Fourier component of w with spatial frequency ϕ will grow at the rate $\lambda(\phi)$ given by equation (4) in the main text. When the transform $\tilde{\alpha}(\phi)$ of the competition kernel $\alpha(x)$ had to be determined numerically, we used the FFTW software package.